Adaptive notch filters from lossless bounded real all-pass functions for frequency tracking and line enhancing

D1.12

Adaptive Notch Filters from Lossless Bounded Real All-Pass Functions for Frequency Tracking and Line Enhancing

Jonathon. A. Chambers and Anthony. G. Constantinides

Department of Electrical Engineering
Imperial College of Science, Technology and Medicine,
Exhibition Road, London, SW7 2BT, UK

ABSTRACT

The objective of this paper is to introduce novel constrained adaptive notch filters which are synthesised from a numerically robust all-pass filter section. This section is realised as a structurally lossless bounded real function which is canonic in both multipliers and delay elements. The new notch filter structures admit orthogonal tuning of their notch frequency and bandwidth. For the two structures, frequency tracking and signal enhancement outputs are derived. Interesting connections are made with the structures that others workers have employed. The mirror image pair of polynomials present in a real all-pass transfer function is shown to yield significant simplification in the generation of the necessary gradient terms used in parameter adaptation. A cascade of such structures is shown to be suitable for tracking multiple sinusoids. Simulation results are included which verify the utility of these new structures for frequency tracking.

1. Introduction

The problem of tracking the frequencies of, and oftentimes to enhance, a number of sinusoidal signals embedded in additive noise has important application in numerous fields, for example in communications, radar and sonar.

One approach to this problem is based on the use of an Adaptive Line Enhancer (ALE) as proposed by Widrow [1]. The ALE has the disadvantage however that it does not possess a direct mechanism for frequency tracking. Therefore, a method for frequency measurement has been suggested which is based on the use of the coefficients of the filter within the ALE to obtain an instantaneous estimate of the power spectrum of the enhanced signal [2]. Such a method of frequency estimation has the disadvantage that it increases considerably the algorithmic complexity of the basic ALE. A further limitation of the conventional Finite Impulse Response (FIR) filter structure of the ALE is that it is not well-suited to modelling a highly selective transfer function as necessary for line enhancing.

Much recent interest has therefore focused on the application of an Adaptive Notch Filter (ANF) to both the problem of frequency tracking and line enhancement [3,4,5,6]. An ANF is chosen because after convergence the frequency response of a conventional ALE, from input to error output, is that of a notch filter and that the notch frequency is generally simply related to a number of the parameters of the ANF which provides a simple mechanism for frequency tracking [3]. Several ANFs must be connected together in order to track or enhance more than one sinusoid. Methods for such connection have been either in a parallel or cascade form but have often suffered from the problem of biased frequency estimates [7]. To overcome this problem it is necessary to minimise the overall output error of a cascade structure, rather than local errors, which leads to an increase in the complexity of the generation of the gradient terms required for the adaptation algorithm.

For example to track N sinusoids Kwan [8] employs a total of N(N+1)/2 + N second-order sections for both the ANFs and to generate the necessary gradient terms. Within this paper two new structures for ANFs are synthesised from a numerically robust all-pass filter section, both of which provide frequency tracking and line enhancing outputs. The second of these new structures when cascaded requires only N(N+1)/2 second-order sections for tracking N sinusoids.

2. All-Pass Function Realisation

The frequency response of an all-pass transfer function has unit magnitude for all ω, i.e. $|H(e^{j\omega})|^2 = 1$ for *all* ω. A stable, real, first-order all-pass function has a transfer function of the form

$$H_{ap1}(z) = \frac{z^{-1} - \beta}{1 - \beta z^{-1}} \ \textit{with} \ |\beta| < 1 \qquad (1)$$

whereas for a stable second-order real all-pass function, with complex poles, it is given by

$$H_{ap2}(z) = \frac{z^{-2} - (1+\alpha)\beta z^{-1} + \alpha}{1 - (1+\alpha)\beta z^{-1} + \alpha z^{-2}} \qquad (2)$$

with $0 < \alpha < 1$ and $\beta^2 < \dfrac{4\alpha}{(1+\alpha)^2}$. The mirror-image pair [9] relationship between the coefficients of the numerators and the denominators of eqns. (1) and (2) is characteristic of all-pass functions. This symmetry is therefore employed to reduce the complexity of the gradient terms necessary for the adaptation of the new ANF structures. The assumption is made that the denominator parameters of the all-pass filter are fixed and only the partial derivative with respect to one of the numerator coefficients is calculated.

An ideal all-pass filter realised in infinite precision is lossless [9]. To realise an all-pass filter various structures are available, however in order to force the transfer function of such a filter to remain all-pass, independent of finite precision effects, a structure which is canonic in multipliers is employed [11]. Such a structure is termed as structurally Lossless Bounded Real (LBR) and is shown in Figure 1. All-Pass functions are also the basis for the frequency transformations developed by Constantinides [11]. Such transformations can not be applied as direct replacements for the delay elements within IIR filters because delay-free loops are introduced. However, another low-pass-to-band-pass all-pass transformation which does not introduce delay-free loops is given by

$$z^{-1} \rightarrow -z^{-1}\frac{(z^{-1} - \beta)}{(1 - \beta z^{-1})} \qquad (3)$$

CH2977-7/91/0000-1553 $1.00 © 1991 IEEE

Through the replacement of z with $e^{j\omega}$ in eqn. (3) the frequency mapping nature of the transformation is revealed

$$\omega_{lp} = \pi + \omega_{bp} + 2\tan^{-1}\left\{\frac{(1+\beta)}{(1-\beta)}\tan\left(\frac{\omega_{bp}}{2}\right)\right\} \qquad (4)$$

from which it is straightforward to show that when $\omega_{bp} = \cos^{-1}(\beta)$ and $\omega_{lp} = 0$, the phase shift produced by the two functions in eqn. (3) is zero.

3. The New Notch Filter Structures

The first ANF structure, henceforth referred to as NFA, is based on a low-pass prototype filter with a transfer function of the form

$$H_{lp}(z) = (1-\alpha)\frac{z^{-1}}{(1-\alpha z^{-1})} \qquad (5)$$

This filter has unity gain and zero phase shift at DC, and the α parameter controls its bandwidth. With the application of the transformation given in eqn. (3) a band-pass filter with the following transfer function is obtained

$$H_{bp1}(z) = (1-\alpha)\frac{z^{-1}(\beta - z^{-1})}{1-(1+\alpha)\beta z^{-1}+\alpha z^{-2}} \qquad (6)$$

This filter has unity gain and zero phase shift at $\omega_{peak} = \cos^{-1}(\beta)$ and has a bandwidth dependent only upon α. The transfer function in eqn. (6) is exactly the same as that used by David [7]. However, to minimise the number of multipliers used in the realisation of eqn. (6), a new structure is proposed based on eqn. (5) with the delay element replaced by the transformation given in eqn. (3) in conjunction with a structurally LBR realisation of the first-order all-pass filter. NFA is formed through the subtraction of the output of the band-pass filter from its input which yields the following transfer function

$$H_{not1}(z) = \frac{1-2\beta z^{-1}+z^{-2}}{1-(1+\alpha)\beta z^{-1}+\alpha z^{-2}} \qquad (7)$$

This transfer function has a notch frequency given by $\omega_{notch} = \cos^{-1}(\beta)$ which provides a convenient mechanism for frequency tracking. The output of the band-pass filter provides a line enhancement output.

The second type of ANF structure, NFB, is composed of a parallel combination of a second-order all-pass filter and a direct connection and is related to the ANF proposed by Friedlander [6]. The overall notch filter response is achieved only by the phase difference between the two paths. The second-order all-pass filter has a transfer function as given in eqn. (2) which leads to a scaled, by a factor of $\frac{(1+\alpha)}{2}$, notch transfer function as given in eqn. (7). Therefore, the same frequency tracking output is available from this second structure. To obtain a line enhancement output it is simply a matter of the inclusion of one additional adder to form the output $H(z) = \frac{1}{2}[1 - H_{ap2}(z)]$ to provide a bilinear band-pass output. The band-pass transfer function which results is

$$H_{bp2}(z) = \frac{(1-\alpha)}{2}\frac{(1-z^{-1})(1+z^{-1})}{1-(1+\alpha)\beta z^{-1}+\alpha z^{-2}} \qquad (8)$$

and is the same as that used by Kwan [8]. Theoretically, for both structures, frequency tracking is unbiased [8]. The two structures permit orthogonal tuning of their notch frequency and bandwidth. The important difference between the use of the two structures is found in the ease with which the necessary gradient terms for the adaptation algorithm are generated.

4. Adaptive Algorithms

The strategy employed for the adaptation of both structures is to pre-set the notch bandwidth, viz. the α parameter, and to adapt only the notch frequency parameter β. Therefore, no stability problems are anticipated during adaptation because the poles of the notch filter are constrained to lie on a circle within and concentric to the unit circle. David *et al.* [12] show that the error performance function is nonuniform and its shape, as a function of β with fixed α, is critically dependent upon the choice of α. Such an error performance function, for the NFB structure, is shown in Figure 2, which corresponds to a single input sinusoid of normalized frequency 0.2 and the signal and noise power levels as used in the first simulation. Therefore, for the adaptive NFA and NFB structures, when a value for α is selected it is important to consider three issues: the effect on the notch bandwidth, the shape of the error performance surface and the range of reachable angular frequencies. The choice of the initial value for the β parameter also has significant effect on the algorithm performance and if a cascade of notch filters is employed to track a number of sinusoids it is advisable to opt for different starting values for each section. In a statistically stationary application it may be advantageous to adapt the α parameter after the appropriate notch frequency is found, so as to narrow the notch bandwidth as in Nehorai's method.

The Normalized Recursive Least Mean Square (NRLMS) algorithm is used to adapt the β parameter due to the nonuniformity of the error performance surface. The NRLMS algorithm for the adaptation of β is

$$\beta_{k+1} = \beta_k - \mu\,\nabla_k / 2\psi_k \qquad (9)$$

$$\nabla_k = \frac{\partial(e_k)^2}{\partial\beta} \qquad (10)$$

$$\psi_k = \gamma\,\psi_{k-1} + (1-\gamma)\left(\frac{\partial(\hat{d}_k)}{\partial\beta}\right)^2 \qquad (11)$$

where γ is a forgetting factor with range $(0 \ll \gamma < 1)$ and μ is the adaptation gain. ψ_k represents a smoothed estimate of the instantaneous power in $\frac{\partial(\hat{d}_k)}{\partial\beta}$. To calculate the appropriate gradient terms each notch filter structure is considered separately. For the NFA structure $e_k = d_k - \hat{d}_k$, therefore

$$\frac{\partial(e_k)^2}{\partial\beta} = -2\,e_k\,\frac{\partial(\hat{d}_k)}{\partial\beta} \qquad (12)$$

The calculation of the derivative, but only with respect to the β in the numerator of the all-pass function, yields

$$\frac{\partial(\hat{d}_k)}{\partial\beta} = \frac{1}{2\pi j}\int_C (1-\alpha)\frac{\dfrac{z^{-1}}{1-\beta z^{-1}}}{\left(1+\alpha z^{-1}\dfrac{z^{-1}-\beta}{1-\beta z^{-1}}\right)^2} \times X(z) z^{k-1}\,dz \qquad (13)$$

which is the expression for the gradient generation filtering illustrated in Figure 3.

For the NFB structure $e_k = d_k + \hat{d}_k$, thus eqn. 12 becomes

$$\frac{\partial(e_k)^2}{\partial\beta} = 2\,e_k\,\frac{\partial(\hat{d}_k)}{\partial\beta} \qquad (14)$$

and the derivative with respect to the numerator β is shown easily to be

$$\frac{\partial(\hat{d}_k)}{\partial\beta} = \frac{1}{2\pi j}\oint_C \frac{1}{2}\frac{-(1+\alpha)z^{-1}}{\left(1-(1+\alpha)\beta z^{-1}+\alpha z^{-2}\right)} \times X(z)z^{k-1}\,dz \qquad (15)$$

Within Figure 4 the complete adaptive NFB structure is shown. With the addition of one extra multiplication the necessary gradient term is generated. A cascade of such structures can be used to track multiple sinusoids and only a total of N(N+1)/2 second-order sections is required for tracking N sinusoids. Importantly, it is the final output error which is minimised by such a cascade of notch filters. The gradient terms calculated in eqns. (13) and (15) can only be approximated in the adaptive realisation since the exact values of β are unknown and must be replaced by their instantaneous estimate β_k.

5. Simulation Results

The frequency tracking simulations are on lines similar to those reported by Kwan [8] and are given as plots of the instantaneous normalized frequency against sample number. For the new ANF structures the plots are achieved using $\frac{1}{2\pi}\cos^{-1}(\beta_k)$. The α parameter is set to 0.9025 which determines the notch bandwidth and the range of reachable frequencies. The input signals consist of a number of sinusoids and zero-mean additive white Gaussian noise. Figure 5 shows the transient responses for the structure due to Kwan, and the NFA and NFB structures, when used to track a single sinusoid with unity power. The input SNR is 10dB and the initial sinusoid frequency is set at 0.15, which after 100 sample points is switched to 0.2. γ is chosen as 0.99 and $\psi_0 = 1.0$. The adaptation gain μ is 0.01 for the NFA structure and 0.0005 for the NFB structure. β_0 is selected to pre-set the notch frequency to be 0.15. The results evidence clearly that both the NFA and NFB structures can track a frequency jump. The track for the NFA is appreciably more noisy due to the additional complexity of its gradient generation. To assess the signal enhancement capabilities of the new structures the SNR improvement ratios (SNRIR) are considered. For the NFA structure the SNRIR is $\frac{(1+\alpha)}{(1-\alpha)}$ whereas $\frac{2}{(1-\alpha)}$ for the NFB structure. As an example, with $\alpha = 0.9025$ the SNRIRs are respectively 19.5 and 20.5. To obtain compatible performance with a conventional ALE a tap-length of the order of 40 is required [1].

As the NFA structure had a smoother track and because it has a simpler gradient structure and the higher SNRIR it is used for the second simulations. Figure 6 shows the result from the cascaded NFA structures when employed to track two sinusoids with disparate powers. These sinusoids are at frequencies of 0.12 and 0.14 with powers of 1.0 and 0.01. The variance of the noise is 0.01 so that the SNRs which correspond to each sinusoid are respectively 20dB and 0dB. The notch filter structures are initialised so that their notch frequencies are 0.1 and 0.11. For the NFB structure μ is set to 0.000125. Only three second-order sections are necessary for the cascade structure based on NFB whilst five would be necessary for the structures due to Kwan.

6. Conclusion

All-pass sections, realised as numerically robust structurally LBR functions, have been employed to provide new structures for constrained ANFs. These new ANF structures can be used for both frequency tracking and line enhancement. Much simplification in the generation of the gradient terms necessary for the adaptive algorithms has been achieved through the utilization of the mirror-image pair of polynomials present in an all-pass function. These new structures can be cascaded to track multiple sinusoids in additive broadband noise. For NFB, with an input of N sinusoids, only N(N+1)/2 second-order sections are necessary for the entire cascade structure. Simulations have verified the suitability of these structures for frequency tracking.

7. Acknowledgement

The UK Science and Engineering Research Council provided funding for this work.

References

[1] **B. Widrow** *et al.*, *Adaptive noise cancelling:Principles and applications*, Proc. IEEE, vol.63, 1975, pp. 1692-1716.

[2] **L.J. Griffiths**, *Rapid measurement of digital instantaneous frequency*, IEEE Trans., vol. ASSP-23, 1975, pp. 207-222.

[3] **D.R. Hush, et al.**, *An Adaptive IIR Structure for Sinusoidal Enhancement, Frequency Estimation, and Detection*, IEEE Trans., vol. ASSP-34, .1986, pp. 1380-1389.

[4] **D.V. Bhaskar Rao and S.Y. Kung**, *Adaptive notch filtering for the retrieval of sinusoids in noise*, IEEE Trans., vol. ASSP-32, 1984, pp. 791-802.

[5] **A. Nehorai**, *A minimal parameter adaptive notch filter with constrained poles and zeros*, IEEE Trans., vol. ASSP-33, 1985, pp. 983-996.

[6] **B. Friedlander and J.O. Smith**, *Analysis and performance evaluation of an adaptive notch filter*, IEEE Trans., vol. IT-30, 1984, pp. 283-295.

[7] **R.A. David**, *Detection of multiple sinusoids using a parallel ALE*, Proc. ICASSP, 1984, pp. 21.2.1-4.

[8] **T.Kwan** and **K. Martin**, *Adaptive Detection and Enhancement of Multiple Sinusoids Using a Cascade IIR Filter*, IEEE Trans., vol. CAS-36, 1989, pp. 937-947.

[9] **P.A. Regalia, S.K. Mitra** and **P.P. Vaidyanathan**, *The digital all-pass filter: a versatile signal processing building block*, Proc. IEEE, vol. 76, 1988, pp. 19-37.

[10] **R.A. Valenzuela** and **A.G. Constantinides**, *Digital signal processing schemes for efficient interpolation and decimation*, IEE Proc. Part G, vol. 130, 1983, pp. 225-235.

[11] **A.G. Constantinides**, *Spectral transformations for digital filters*, Proc. IEE, vol. 117, 1970, pp. 1585-1590.

[12] **R.A. David, S.D. Stearns, G.R. Elliott and D.M. Etter** *IIR algorithms for adaptive line enhancement*, Proc. ICASSP, 1983, pp. 1.5.17-20.

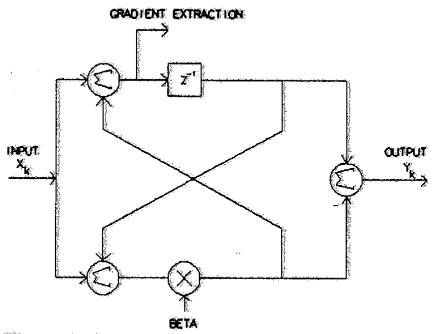

Figure 1 First-Order Stucturally LBR All-Pass Function H_{ap1}.

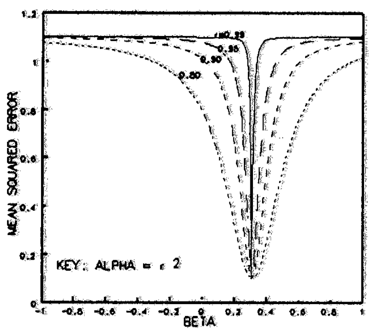

Figure 2 Error Performance Function

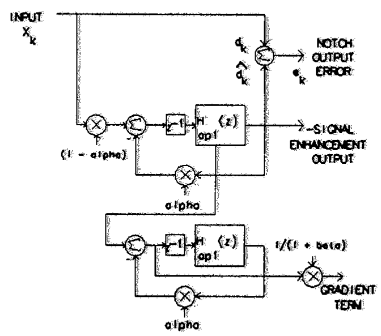

Figure 3 Complete Adaptive NFA Structure

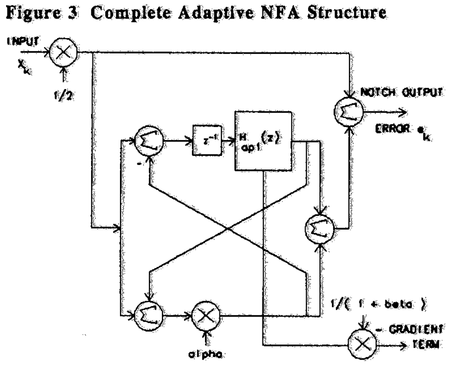

Figure 4 Complete Adaptive NFB Structure

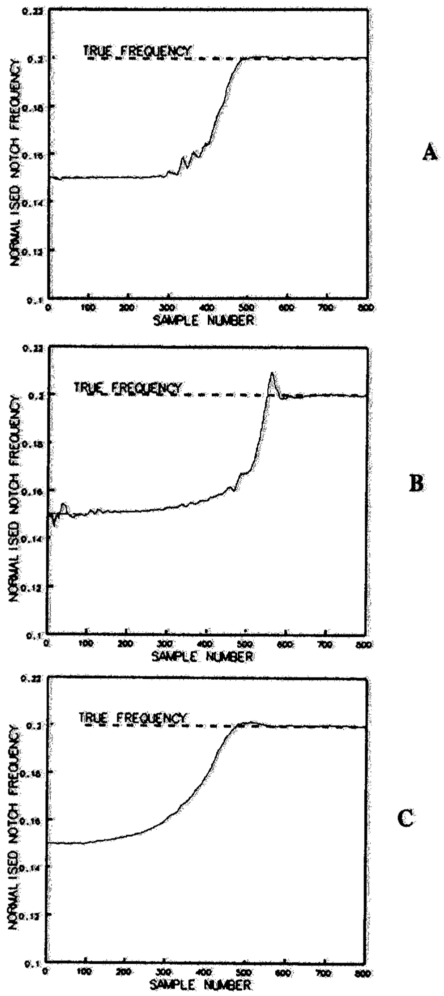

Figure 5 Instantaneous Frequency Tracks
a:Obtained from Structure of Kwan
b:Obtained from NFA Structure
c:Obtained from NFB Structure

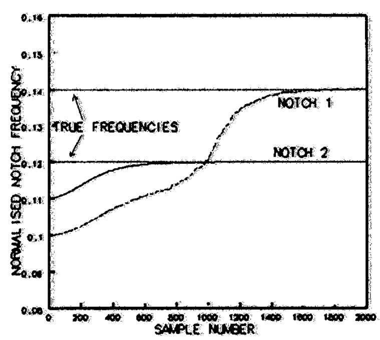

Figure 6 Instantaneous Frequency Tracks Obtained from NFB Structure